

Heat conductivity in the presence of a quantized degree of freedom

JUN-WEN MAO^{1,2}(*) and YOU-QUAN LI¹

¹ *Zhejiang Institute of Modern Physics, Zhejiang University, Hangzhou 310027, P.R. China.*

² *Department of Physics, Huzhou Teachers College, Huzhou 313000, P.R. China.*

PACS. 44.10.+i – Heat conduction .

PACS. 05.45.-a – Nonlinear dynamics and nonlinear dynamical systems.

PACS. 05.70.Ln – Nonequilibrium and irreversible thermodynamics.

Abstract. – We propose a model with a quantized degree of freedom to study the heat transport in quasi-one dimensional system. Our simulations reveal three distinct temperature regimes. In particular, the intermediate regime is characterized by heat conductivity with a temperature exponent γ much greater than 1/2 that was generally found in systems with point-like particles. A dynamical investigation indicates the occurrence of non-equipartition behavior in this regime. Moreover, the corresponding Poincaré section also shows remarkably characteristic patterns, completely different from the cases of point-like particles.

The problem of heat conduction in low-dimensional systems has been an interesting subject for a long time due to the potential applications of nanostructured materials and the importance in understanding the physics of low-dimensional systems (see review [1] and the references therein). A long standing issue is the exploration of the necessary condition for a dynamical system to obey the Fourier law [2–6]. For this purpose, a class of “Billiard gas channel” has been proposed recently [7–10] to investigate the connection between macroscopic heat transport and microscopic dynamics. In these models, usually a series of scatterers are placed periodically along two parallel walls, and point-like particles without interaction frequently undergo specular reflections on the boundary formed by the scatterers and the walls. By tracing the motion of the particles, the energy transport in a periodic structure is investigated. Despite intensive simulations in recent years, the sufficient condition for a dynamic system ensuring the Fourier law is still not clear. For example, it was ever found that the system with positive Lyapounov exponent [7] obeys the Fourier law, while the same result was obtained in some linear mixing systems with zero Lyapounov exponent [8–10]. Recently, a modified Lorentz model where particles collide with fixed freely-rotating scatterers was suggested to investigate the heat transport in local thermal equilibrium [11, 12]. Normal transport is obtained in such system, indicating that the transport coefficients are finite in the thermodynamic limit.

(*) E-mail:jwmao@zimp.zju.edu.cn

Although these simple models provide a framework in which heat transport emerges, they assume point-like particles (heat carriers), and fail to provide a clear understanding of temperature effects on heat transport. In fact, along with the dramatic achievements in nanotechnology, the control of heat transport for nanoscopic devices becomes increasingly important. Thus, it is crucial to understand the temperature dependence of heat conductivity in low dimensional system. Since the billiard model captures the underlying dynamics of the system, it will be appropriate for us to study the heat conductivity from the microscopic dynamic point of view.

In this paper we propose a simple model to study the heat transport, which demonstrates different regimes in the heat conductivity. We consider a quasi-one-dimensional billiard gas channel in which the heat carriers possess an additional (intrinsic) quantized degree of freedom (e.g., rotational velocity) beyond two translational ones. In general, this kind of degree of freedom can come from the composite nature of the carriers, or from the confinement in a third dimension. We explore the scattering of the particles with rough surfaces (modeled by fixed half disks). Here we focus on inelastic events and take no account of the energy or the momentum exchange between the particles and the scatterers. Namely, a collision with the rough surface involves the occurrence of energy transfer between the translational and the rotational degrees of freedom. Our simulations show that there are three regimes according to the temperature exponent γ in the heat conductivity $\kappa \sim T^\gamma$. The transition from high temperature regime to intermediate temperature regime occurs close to a characteristic temperature T_c , below which the translational velocity distribution deviates from the Boltzmann distribution while energy is distributed unequally among the three degrees of freedom. In addition, by plotting the Poincaré section we find the clear emergence of strange attractor accompanying the frozen of rotation degree of freedom at low temperatures.

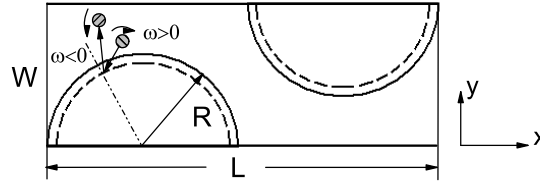


Fig. 1 – Schematic of the collision of a particle of radius r with a scatterer in a unit cell of the channel. The surface of the semicircle scatterers are plotted by dashed lines, near which the solid lines are the surrounding tracks of the center of particles when colliding with the scatterers. In the calculations, $L = 3.6a$, $W = 1.0392a$, $R = 0.89a$ and $r = 0.01a$.

In our model, the channel in x direction consists of two parallel walls of distance W (Figure 1 shows the unit cell of the channel). A series of semicircle scatterers with radius R are placed periodically along two horizontal walls. Each cell has two semicircles, one on the bottom, the other on the top. The heat baths at two terminals of the channel are modelled by stochastic kernels of Gaussian type [9],

$$\begin{aligned} P(v_x) &= \frac{m|v_x|}{k_B T} \exp\left(-\frac{mv_x^2}{2k_B T}\right), \\ P(v_y) &= \sqrt{\frac{m}{2\pi k_B T}} \exp\left(-\frac{mv_y^2}{2k_B T}\right), \end{aligned} \quad (1)$$

which determines the translational velocity v_x and v_y of the particles in the channel after colliding with the walls between the channel and the heat baths.

The particle with radius r has a rotational velocity ω in addition to the conventional velocities v_x and v_y which describe the particle's translational movement. Since each unit cell contributes only one heat carrier whose radius is small compared with the scale of the channel, the interaction between the particles is not taken into account for simplicity. Under the assumption of $v'_\perp = -v_\perp$, the conservations of energy and angular momentum read

$$\frac{1}{2}mv'^2 + \frac{1}{2}I\omega'^2 = \frac{1}{2}mv_\parallel^2 + \frac{1}{2}I\omega^2, \quad (2)$$

$$mr v'_\parallel + I\omega' = mr v_\parallel + I\omega, \quad (3)$$

where the primed and unprimed ones represent the quantities after and before a collision; the v_\parallel and v_\perp refer to the components tangential and perpendicular to the scatterer surface, respectively. The moment of inertia around an axis through the center of a particle of mass m is $I = \alpha mr^2$. The similar collision rule has been appeared in [11, 12]. Note that in our model α ranging from 0 to 1 measures the moment of inertia, which corresponds to the mass distribution of the disk particle, i.e., $\alpha = 0$ for point particles, $1/2$ for uniform distributed mass. Eqs. (2) and (3) lead to the following solution:

$$\begin{pmatrix} v'_\perp \\ v'_\parallel \\ \omega' r \end{pmatrix} = \begin{pmatrix} -1 & 0 & 0 \\ 0 & \frac{1-\alpha}{1+\alpha} & \frac{2\alpha}{1+\alpha} \\ 0 & \frac{2}{1+\alpha} & -\frac{1-\alpha}{1+\alpha} \end{pmatrix} \begin{pmatrix} v_\perp \\ v_\parallel \\ \omega r \end{pmatrix}. \quad (4)$$

In addition to the specular reflections with the parallel walls, the collision rules of semicircles are described as above equation. Both the translational and the rotational velocities are changed after a collision owing to the friction force against the total tangential velocity of the contact point at the surface of the particle (ball).

The rotational degree of freedom naturally introduces the quantization condition $I\omega_l = l\hbar$, $l = 0, \pm 1, \pm 2, \dots$ which is well known for angular momentum in quantum mechanics. Clearly, the moment of inertia determines the spacing of the quantized angular velocity $\Delta\omega = \hbar/I = \hbar/\alpha mr^2$, and the energy spacing $\hbar^2/\alpha mr^2$ between the ground state and the first excited state defines a characteristic temperature $T_c = \hbar^2/\alpha mr^2 k_B$. Actually, the rotational part can be regarded as an intrinsic degree of freedom, then our model itself manifests internal excitations. If the energy for such excitation is much less than $k_B T_c$, the internal degree of freedom is frozen. In our simulations, the particle's $\tilde{\omega}$ takes an allowed discrete value near the ω' given by eq. (4). Under this assumption, the conservation of angular momentum is broken down, for the tangential component of velocity \tilde{v}_\parallel is the same as v'_\parallel , while the perpendicular component \tilde{v}_\perp is determined by the energy conservation. In the simulation process, we set the parameter a , the particle mass m , Boltzmann constant k_B and Planck's constant \hbar as unity for convenience.

As the quantized degree of freedom is assumed to play the role in the channel, the rotational velocity then does not change when a particle in the channel is rebounded from the walls of two heat baths. The heat flux is calculated by the exchange of energy carried by the particles via the collisions with a heat bath within total time t_M spent for M such collisions [8],

$$J = \frac{1}{t_M} \sum_{j=1}^M (\Delta E)_j, \quad (5)$$

where $(\Delta E)_j = (E_{in} - E_{out})_j$ is the energy exchange at the j th collision with a heat bath. Note that above heat flux is for a single particle. In the channel with N cells, the heat conductivity is found to be $\kappa = JN^2L/\Delta T$.

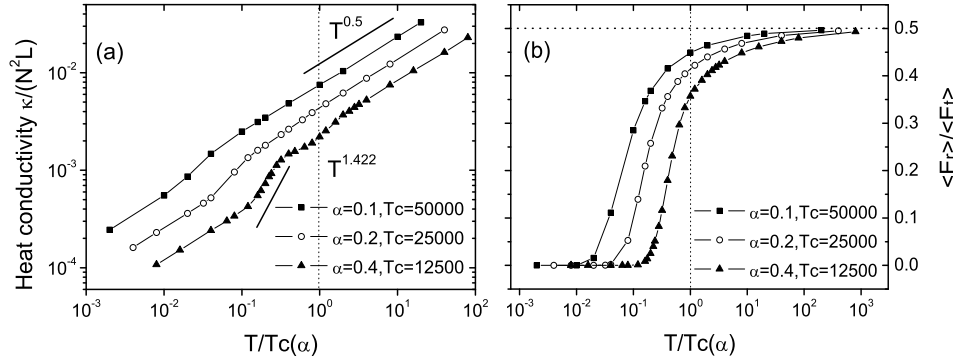


Fig. 2 – (a) Temperature dependence of heat conductivity. (b) The ratio of average rotational energy over average translational energy at different temperatures. The calculations are made for $\alpha = 0.1, 0.2$, and 0.4 .

Figure 2(a) shows the heat conductivity-temperature curves for a channel with $N = 32$ cells. Here $T_c = 5000/\alpha$ (in units of $\hbar^2/mk_B a^2$). Because of non-equipartition of energy in the system, which we will discuss next, one can not define a local temperature from microscopic point of view. For simplicity, we assume an average value of temperature $T = (T_L + T_R)/2$ under small temperature gradient, where T_L and T_R are the temperatures of two heat baths respectively. The temperature difference $\Delta T/T$ is fixed at 0.2. To obtain the heat conductivity correctly, we investigated heat flow J in Eq.(5) as a function of temperature gradient in a wide range of 5 orders of magnitude, as was done in ref. [13]. We have verified the linear relation of $J \sim \nabla T$ for temperatures and gradient explored in fig. 2. One can clearly see that the curves have larger slope at temperatures near and less than T_c . Our calculations exhibit that the maximum value of the slope reaches 1.422 for the case of $\alpha = 0.4$.

To illustrate this characteristic, we investigate the average translational energy $\langle E_t \rangle_i$ and the rotational energy $\langle E_r \rangle_i$ in a unit cell

$$\langle E_\sigma \rangle_i = \frac{\sum_{j=1}^M t_{ij} (E_\sigma)_{ij}}{\sum_{j=1}^M t_{ij}}, \quad \sigma = t, r. \quad (6)$$

where $E_t = \frac{1}{2}mv^2$ and $E_r = \frac{1}{2}I\omega^2$, i represents the i th cell and t_{ij} is the time spent within the cell for the j th visit. In fig. 2(b) we plot the ratio of $\langle E_t \rangle / \langle E_r \rangle$, where $\langle E_t \rangle$ and $\langle E_r \rangle$ are the translational and the rotational energies averaging over N cells, respectively. Clearly, there are three regimes with different characteristics.

1. Low temperature limit: Our simulations exhibit $\kappa \sim T^\gamma$ with $\gamma \sim 1/2$ for various values of α at low temperatures (shown in fig. 2(a)). This coincides with the result in previous literature [8]. We also calculate the temperature exponent γ for the model of [7] and [14], respectively, obtaining the result $\gamma \sim 1/2$ again. In the following we make an estimation of the heat conductivity κ . In fact, at low temperatures $T \ll T_c$, the heat carriers in our model can be regarded as point-like particles because their thermal energy $k_B T$ is much smaller than the first excitation energy. In this case, the rotational motions are frozen. The heat conductivity is estimated as $\kappa \sim \lambda \langle |\tilde{v}| \rangle$ where λ is the mean free path and $\langle |\tilde{v}| \rangle$ describes the average absolute velocity [15]. For ideal gas it follows that $\langle |\tilde{v}| \rangle \sim \sqrt{2k_B T/m}$. Consequently, we have $\kappa \sim T^{1/2}$ when λ is treated as a constant.

2. Intermediate temperature regime: The abrupt increase for the curves in fig. 2(a) in the intermediate temperature regime is related to the presence of quantized rotational degree of freedom. It seems that the less moment of inertia the particle possesses, the further the abrupt increasing regime is away from its characteristic temperature. As is shown in fig. 2(b), the ratio $\langle E_t \rangle / \langle E_r \rangle$ rises rapidly from zero with increasing temperature T till T_c , then asymptotically to 1/2. This indicates that the total energy of the system is not equally partitioned among the three degrees of freedom except in high temperature limit. As a result, the temperature dependence of the average velocity $\langle |\tilde{v}| \rangle$ is significantly affected by the ratio of the translational kinetic energy to the total energy, which seems to be responsible for the abrupt increase of heat conductivity since κ is proportional to $\langle |\tilde{v}| \rangle$. The non-equipartition of energy, which has been studied in granular mixtures [16–18], has now been observed in our model due to non-conservation of angular momentum.

3. High temperature limit: In high temperature limit, the saturation of the value of $\langle E_t \rangle / \langle E_r \rangle$ is observed. In this case, the quantum effect are almost overwhelmed by the thermal fluctuations and thus the macroscopic system is in thermodynamic equilibrium. The curves in fig. 2(a) show γ goes back to 1/2 again, however, the underlying mechanism is quite different.

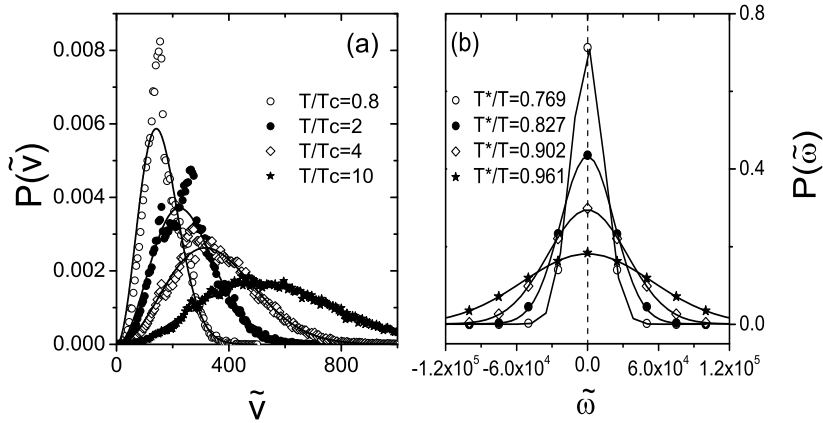


Fig. 3 – Probability distribution at temperatures $T/T_c = 0.8$ (○), 2 (●), 4 (◇), and 10 (★) for $\alpha = 0.4$ and $N = 8$. (a) The translational velocity distribution. Solid lines are the Boltzmann distributions at the corresponding temperatures. (b) The rotational velocity distribution. The T^* is obtained by the best fits (solid lines) of Gaussian distribution for numerical data.

In the non-equilibrium regime, the traditional definition of temperature can not well describe the features of the system. To understand the characteristics of these regimes further, we measure the translational velocity distribution $P(\tilde{v})$ and the rotational velocity distribution $P(\tilde{\omega})$ of the particles. The simulation is performed in a equilibrium system of $T_L = T_R$, where 10^5 particles with initial Gaussian distribution of velocity at a certain temperature T are put into the channel to make collisions with the semicircle rough surfaces, while undergoing specular reflections with the straight walls. After a long relaxation time, the system reaches a steady state. As shown in fig. 3(a), solid lines are the Boltzmann distributions in equilibrium at the corresponding temperatures. Better agreements appear when $T/T_c \geq 10$, which indicates that the particles can be considered as the classical ideal gas in equilibrium in the high temperature limit despite the existence of quantized rotational velocity. In com-

parison to the velocity distribution at relatively low temperatures, the deviations from the Boltzmann distribution are evident, leading to a larger average velocity. Figure 3(b) shows the rotational velocity distributions $P(\tilde{\omega})$, which are typical Gaussian distributions. T^* is the best fits of the curves. As expected, it is lower than the given temperature. The result of $T^*/T \rightarrow 1$ with increasing temperature till the high temperature limit shows that the system is asymptotically close to equilibrium state.

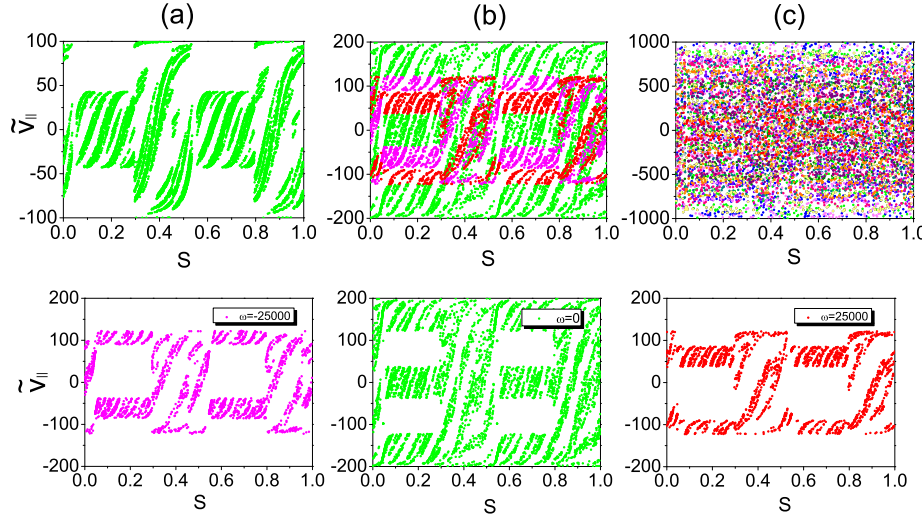


Fig. 4 – (Color online) Poincaré surface of section projected to $s - \tilde{v}_{\parallel}$ plane, by following the first 10^4 bounces with zero initial angular velocity. The particle of velocity v and $\alpha = 0.4$ starts from the center of the left boundary of the cell with an incident angle of 0.9. (a) $v = 100$, and the allowed $\tilde{\omega} = 0$; (b) $v = 200$, and the allowed $\tilde{\omega} = -25000, 0$, and 25000 ; (c) $v = 1000$, and more values of $\tilde{\omega}$ are allowed. Additionally, the Poincaré surfaces of section for $\tilde{\omega} = -25000, 0$ and 25000 at $v = 200$ are displayed on the second row, respectively.

To capture the physics of our model, we investigate the Poincaré surface of section (SOS) which has been employed to characterize the microscopic dynamics for the motion of a point-like particle colliding with the boundary [19]. It is thus natural to investigate the dynamical characteristics of the system in the presence of quantized degree of freedom. Using our previous strategy [14], we treat one unit cell of the channel and close the two ends by straight frictionless walls. Particles with certain initial velocity are injected into the cell, then they collide with the boundary. The SOS in our model is defined as $(s, \tilde{v}_{\parallel}, \tilde{\omega})$ where s is the distance to the starting site along the boundary, \tilde{v}_{\parallel} the tangential component of translational velocities and $\tilde{\omega}$ the rotational velocity of the particle. By projecting the points in phase space to the $s - \tilde{v}_{\parallel}$ plane, we plot the Poincaré surface of section $(s, \tilde{v}_{\parallel})$ where different values of rotational velocity $\tilde{\omega}$ are displayed in different colors. In our simulations, the initial incident angle brings about minor effects on the SOS. Figure 4 (a), (b), and (c) show three distinct cases of $v = 100, 200$, and 1000 , respectively. As a comparison, we investigate the SOS for particles with a classical rotational degree of freedom and find it is filled with widely dispersed points. For the case of $v = 100$ (shown in figs. 4(a)), the rotational velocity is frozen, thus the points are confined in the plane $\tilde{\omega} = 0$. Comparing the pattern with that of classical situation, we note that many areas are eclipsed. The remained pattern implies the existence

of a fractal attractor [20, 21]. This is completely in agreement with what occurred in Bohr model of atoms. As is known that the admissible orbits of an electron moving in the Coulomb field of nucleus occupy the whole phase space. The Bohr-Sommerfeld quantization condition excludes many of the classically admissible orbits, which results in the emergence of eclipse in phase space. When $v = 200$, the rotational velocity is excited and the allowed $\tilde{\omega}$ takes the values of -25000 , 0 , and 25000 . The corresponding SOS are shown in the bottom panels of fig. 4. The points are dispersed in the three layers and form characteristic patterns in each layer. For the case of $v = 1000$, more excited states of higher rotational energy are allowed, as shown in fig. 4(c), and the points at different $\tilde{\omega}$ are randomly dispersed.

In summary, we have proposed a method to introduce the quantized degree of freedom for the first time in the study of heat transport in the billiard channel. We have demonstrated three characteristic regimes for heat conductivity in the presence of quantized degree of freedom. Our results show that the temperature-dependent interplay between the translational and rotational degrees of freedom plays a crucial role in heat conduction. We have also investigated the dynamical properties in these regimes. The non-equipartition of energy between the translational and rotational degrees of freedom is explicitly shown except in the high temperature limit, and strange attractor occurs remarkably in the low temperature limit. We expect that our model provides a strategy to study the effects of the quantized degree of freedom on heat transport.

J.W. Mao thanks X. Wan for helpful discussion and critical remarks on an earlier version of this paper. This work is supported by NSFC No. 10225419 and HZNSF No. 2005YZ03.

REFERENCES

- [1] LEPRI S., LIVI R. and POLITI A., *Phys. Rep.*, **377** (2003) 1.
- [2] CASATI G., FORD J., VIVALDI F. and VISSCHER W. M., *Phys. Rev. Lett.*, **52** (1984) 1861.
- [3] KABURAKI H. and MACHIDA M., *Phys. Rev. Lett.*, **181** (1993) 85.
- [4] LEPRI S., LIVI R. and POLITI A., *Phys. Rev. Lett.*, **78** (1997) 1896.
- [5] LEPRI S., LIVI R. and POLITI A., *EuroPhys. Lett.*, **43** (1998) 271.
- [6] NARAYAN O. and RAMASWAMY S., *Phys. Rev. Lett.*, **89** (2002) 200601.
- [7] ALONSO D., ARTUSO R., CASATI G. and GUARNERI I., *Phys. Rev. Lett.*, **82** (1999) 1859.
- [8] LI B., WANG L. and HU B., *Phys. Rev. Lett.*, **88** (2002) 223901.
- [9] LI B., CASATI G. and WANG J., *Phys. Rev. E.*, **67** (2003) 021204.
- [10] ALONSO D., RUIZ A. and VEGA I. DE, *Phys. Rev. E.*, **66** (2002) 066131; *Physica D*, **187** (2004) 184.
- [11] MEJA-MONASTERIO C., LARRALDE H., and LEYVRAZ F., *Phys. Rev. Lett.*, **86** (2001) 5417;
- [12] LARRALDE H., LEYVRAZ F. and MEJA-MONASTERIO C., *J. Stat. Phys.*, **113** (2003) 197;
- [13] AOKI K. and KUSNEZOV D., *Phys. Rev. Lett.*, **86** (2001) 4029.
- [14] MAO J. W., LI Y. Q. and JI Y. Y., *Phys. Rev. E*, **71** (2005) 061202.
- [15] GENDELMAN O. V. and SAVIN A. V., *Phys. Rev. Lett.*, **92** (2004) 074301.
- [16] GARZO V. and DUFTY J., *Phys. Rev. E*, **60** (1999) 5706.
- [17] FEITOSA K. and MENON N., *Phys. Rev. Lett.*, **88** (2002) 198301.
- [18] DAHL S. R., HRENYA C. M., GARZO V. and DUFTY J. W., *Phys. Rev. E*, **66** (2002) 041301.
- [19] BERRY M. V., *Euro. J. Phys.*, **2** (1981) 91.
- [20] KLAGES R., RATEITSCHAK K. and NICOLIS G., *Phys. Rev. Lett.*, **84** (2000) 4268.
- [21] DELLAGO CH., GLATZ L. and POSCH H. A., *Phys. Rev. E*, **52** (1995) 4817.